Electrophysiological and Electroanatomic Characterization of the Atria in Sinus Node Disease
Evidence of Diffuse Atrial Remodeling

Prashanthan Sanders, MBBS, PhD; Joseph B. Morton, MBBS, PhD; Peter M. Kistler, MBBS;
Steven J. Spence, ACCT; Neil C. Davidson, MD; Azlan Hussin, MBBS; Jitendra K. Vohra, MD;
Paul B. Sparks, MBBS, PhD; Jonathan M. Kalman, MBBS, PhD

Background—The normal sinus pacemaker complex is an extensive structure within the right atrium. We hypothesized that patients with sinus node disease (SND) would have evidence of diffuse atrial abnormalities.

Methods and Results—Sixteen patients with symptomatic SND and 16 age-matched controls were studied. The following were evaluated: effective refractory periods (ERPs) from the high and low lateral right atrium (RA), high septal RA, and distal coronary sinus (CS); conduction time along the CS and lateral RA; P-wave duration; and conduction at the crista terminalis. Electroanatomic mapping was performed to define the sinus node complex and determine regional conduction velocity, double potentials, fractionated electrograms, regional voltage, and areas of electrical silence. Patients with SND demonstrated significant increase in atrial ERP at all right atrial sites, increased atrial conduction time along the lateral RA and CS, prolongation of the P-wave duration, and greater number and duration of double potentials along the crista terminalis. Electroanatomic mapping demonstrated the sinus node complex in SND to be more often unicentric, localized to the low crista terminalis at the site of the largest residual voltage amplitude. There was significant regional conduction slowing with double potentials and fractionation associated with areas of low voltage and electrical silence (or scar).

Conclusions—SND is associated with diffuse atrial remodeling characterized by structural change, conduction abnormalities, and increased right atrial refractoriness. There was a change in the nature of sinus pacemaker activity with loss of the normal multicentric pattern of activation, caudal shift of the pacemaker complex, and abnormal and circuitous conduction around lines of conduction block. (*Circulation*. 2004;109:1514-1522.)

Key Words: sinoatrial node ■ arrhythmia ■ atrium ■ fibrillation ■ pacemakers

S inus node disease (SND) is a common indication for permanent cardiac pacing in the community. It results from disordered impulse generation within the sinus node or impaired conduction of the impulse to the surrounding atrial tissue, thus leading to the clinical manifestation of bradycardia.[1] The natural course of the condition can be of recurrent syncope, heart failure, stroke, and atrial fibrillation (AF).

The unique anatomic[2] and functional[3–6] characteristics of the normal sinus node have been well characterized. Boineau et al[6] made the seminal observation that the sinus P wave could arise from a pacemaker complex distributed over an area extending from the junction of the superior vena cava (SVC) and right atrial appendage in the inferior direction along the sulcus terminalis almost to the inferior vena cava (IVC). Although the normal sinus pacemaker complex phys-

iology has been well characterized, the nature of the atrial pathophysiology that develops in patients with SND has not been documented. Previous studies in SND have focused on the electrophysiological parameters such as sinus node recovery time (SNRT), measurement of sinus node refractoriness, and also on localized conduction measurements such as that provided by the sinus node electrogram but have not characterized the atrial electrophysiology of this condition. The advent of electroanatomic mapping has provided unique insights into atrial pathophysiology in a range of conditions.[7–9]

The present study was designed to determine the electrophysiological and electroanatomic properties of the atria in patients with SND compared with age-matched controls. We hypothesized that given the widely distributed nature of the functional sinus pacemaker complex and the frequent asso-

TABLE 1. Patient Characteristics

	SND (n=16)	Controls (n=16)	P
Age, y	68±9	65±7	NS
Sex, n, male/female	8/8	9/7	NS
LA diameter, mm	40.6±6.6	33.8±4.1	0.0008
LVEDD, mm	48.5±5.9	46.5±5.1	NS
LVESD, mm	29.4±4.3	28.1±5.4	NS
LVFS, %	38.3±7.7	40.0±8.2	NS
Hypertension, n (%)	3 (19)	0	NS
Coronary artery disease, n (%)	4 (25)	0	NS

LA indicates left atrial; LVEDD, left ventricular end-diastolic diameter; LVESD, left ventricular end-systolic diameter; and LVFS, left ventricular fractional shortening.

ciation of SND with AF, patients with SND would have widespread atrial abnormalities.

Methods

Study Population
The study population comprised 16 patients with SND requiring pacemaker implantation. Patients were excluded from the study if they had recent myocardial infarction (≤3 months), ongoing cardiac ischemia, heart failure, valvular heart disease, or atrial arrhythmia. Another 16 age-matched patients having radiofrequency ablation for atrioventricular nodal reentrant tachycardia or atrioventricular reentrant tachycardia without evidence of structural heart disease or history of AF were also studied (Table 1). All medications were suspended >5 half-lives before the study. No patient received amiodarone in the 6 months before the study. All patients gave written informed consent for the study, which was approved by the Clinical Research and Ethics Committee of the Royal Melbourne Hospital.

SND Definition
All patients included in the study had symptoms of cardiac syncope or presyncope associated with either (1) unexplained sinus brady-cardia (<40 bpm; n=8) or (2) prolonged sinus pauses (>3.0 seconds; n=8).

Electrophysiological Study
Electrophysiological study was performed in the postabsorptive state with sedation with midazolam and with autonomic blockade as previously described.[10] Multipolar catheters were positioned as follows: (1) 10-pole catheter with 2-5-2–mm interelectrode spacing in the coronary sinus (CS) with the proximal electrode pair positioned at the CS ostium; (2) 20-pole catheter with 2-5-2–mm interelectrode spacing along the lateral right atrium (RA), positioned ensuring that the first 10 electrodes were linearly arranged along the lateral RA border; (3) 8-pole catheter with 2.5-5-2.5–mm interelectrode spacing along the high septal RA; (4) 20-pole "crista" catheter with 1-3-1–mm interelectrode spacing positioned along the crista terminalis with the aid of a long sheath to ensure stability and assist with its placement in close apposition to the crista terminalis. The catheter position was standardized such that the second bipole lay at the junction of the SVC with the RA as determined by intracardiac echocardiography. The intracardiac echocardiography imaging system consists of a 9-MHz rotating ultrasound transducer mounted at the tip of a 9F catheter.

Surface ECG and bipolar endocardial electrograms were monitored continuously and stored on a computer-based digital amplifier/recorder system with optical disk storage for offline analysis. Intracardiac electrograms were filtered from 30 to 500 Hz and measured with computer-assisted calipers at a sweep speed of 400 mm/s.

Sinus Node Function
The corrected SNRT (CSNRT) was assessed at cycle lengths (CLs) of 600, 500, and 400 ms after a 30-second pacing train and determined as the time from the stimulus artifact to the earliest activity along the crista terminalis. The CSNRT was repeated 3 times at each CL and averaged.

Effective Refractory Period
Atrial effective refractory periods (ERPs) were evaluated at twice diastolic threshold (for a pacing threshold of <2 mA) at CLs of 600, 500, and 400 ms. An incremental technique was used, starting with an S2 coupling interval of 150 ms, which was increased in increments of 5 ms. The ERP was defined as the longest coupling interval failing to propagate to the atrium. ERP was measured from the distal CS, low lateral RA, high lateral RA, and the high septal RA 3 times during each CL at each site. If the maximum and minimum measurements differed by >10 ms, 2 more measurements were taken, and the total was averaged. Heterogeneity of ERP was determined by the coefficient of variation of ERP at each CL (SD/mean×100%).

Atrial Conduction
Conduction time was assessed along the CS by pacing from the distal bipole (1-2) of the CS catheter and measuring time to activate the proximal bipole (9-10), and along the lateral RA by pacing from the distal bipole (1-2) of the lateral RA catheter and measuring time to activate bipole 9-10. At both sites, conduction was measured at pacing CLs of 600, 500, and 400 ms during stable capture. Conduction time was determined 10 times at each CL and averaged.

P-wave duration in sinus rhythm was analyzed as a surrogate marker of interatrial conduction time. P-wave duration was measured from lead II of the surface ECG and averaged from a series of 10 consecutive beats.

Anatomically Determined Conduction Delay
Anatomically determined conduction delay at the crista terminalis was assessed during pacing from the high lateral RA, low lateral RA, and high septal RA at a CL of 600 ms and during the earliest extrastimulus that conducted to the atrium from each of the above sites. Conduction delay was analyzed on each recording bipole of the crista catheter and defined as the presence of discrete double potentials (DPs) separated by an isoelectric interval. Both the number of bipoles demonstrating discrete DPs and the maximum interpotential duration were evaluated. To fully explore the functional properties of the conduction across the crista terminalis, decremental extrastimuli were delivered at the high lateral RA at a CL of 600 ms until ERP was reached (10-ms decrements from an S2 of 350 ms).

Electroanatomic Mapping
Electroanatomic (CARTO) maps of the RA were created either during distal CS pacing or in sinus rhythm (in patients with P-wave morphology consistent with a sinus origin). The system records the 12-lead ECG and bipolar electrograms filtered at 30 to 400 Hz from the mapping catheter and the reference electrogram.

Fluoroscopy, the CARTO system, and intracardiac echocardiography were used to facilitate mapping of anatomic structures, particularly the crista terminalis, and for ensuring endocardial contact when individual points were acquired. High-density mapping was performed along the crista terminalis, septal RA, and areas of low voltage. Points were acquired if the stability criteria in space (≤6 mm) and local activation time (≤5 ms) were met. Editing of points was performed offline. Local activation was manually annotated to the beginning of the first rapid deflection from the isoelectric line on bipolar electrograms. Points were excluded if they did not conform to the 12-lead ECG P-wave morphology or if they were <75% of the maximum voltage of the preceding electrogram. For

the purposes of the electroanatomic map, the following definitions were used: (1) fractionated signals (FS)-complex electrograms of long duration (≥50 ms)[8]; (2) DPs separated by an isoelectric interval,[8] with activation time annotated at the largest potential; (3) electrically silent areas (scar), absence of recordable activity or a bipolar voltage amplitude ≤0.05 mV[8]; and (4) low-voltage areas, contiguous areas ≤0.5 mV on bipolar voltage maps.

Sinus Node Complex and Atrial Propagation

The distance between the SVC-RA junction and the most cranial pacemaker activity was determined as the linear distance between these points. For the purposes of evaluating the sinus node complex, the following definitions were assigned: (1) unicentric: a single source of activation that spreads to activate the atria, and (2) multicentric: ≥2 sites of early activation with activation time difference of ≤5 ms separated by a distance of ≥10 mm.[6]

Atrial propagation was qualitatively assessed and described using anatomically correct nomenclature. The propagation time between the earliest sinus pacemaker complex and the IVC-RA junction and to the earliest activation along the septal RA was determined by the difference in the activation times between these points, respectively.

Regional Conduction Velocity

The CARTO system determines the conduction velocity between 2 points by expressing the linear distance between the points as a function of the difference in activation times. To determine regional conduction velocity, isochronal maps of the atria were created at 5-ms intervals in activation during atrial pacing. Conduction velocity was determined at the high and low septal RA, the high and low lateral RA, and the high and low posterior RA by an average of the conduction velocity between 5 pairs of points along the activation front through the areas of least isochronal crowding.

Atrial Voltage

RA bipolar voltage amplitude was determined during atrial pacing, at the high and low septal RA, the high and low lateral RA, and the high and low posterior RA. At each of these regions, a mean of 10 representative points were evaluated. An index of heterogeneity of bipolar voltage amplitude was obtained by calculating the coefficient of variation of voltage of all points.

Statistical Analysis

All variables are reported as mean±SD. Sequential data measurements were analyzed by ANOVA followed by the Newman-Keuls test for multiple comparisons. Comparison between groups was performed with either Student's t test or the Wilcoxon rank sum test. Proportions were compared by Fisher's exact test. Statistical significance was established at a value of $P < 0.05$.

Results

Patient Characteristics

The 2 groups were age-matched with comparable left ventricular dimensions and function (Table 1). However, patients with SND had significantly larger left atria ($P = 0.0008$).

Sinus Node Function

The CSNRT was significantly prolonged in patients with SND compared with controls ($P < 0.0001$): at 600 ms, 858±364 versus 262±82 ms ($P < 0.01$); at 500 ms, 960±463 versus 289±67 ms ($P < 0.01$); and at 400 ms, 978±450 versus 273±81 ms ($P < 0.01$).

Atrial Refractoriness

ERPs were prolonged in patients with SND compared with controls at all RA sites evaluated ($P < 0.0001$; Figure 1). Within the RA, this did not reach significance only at a CL of
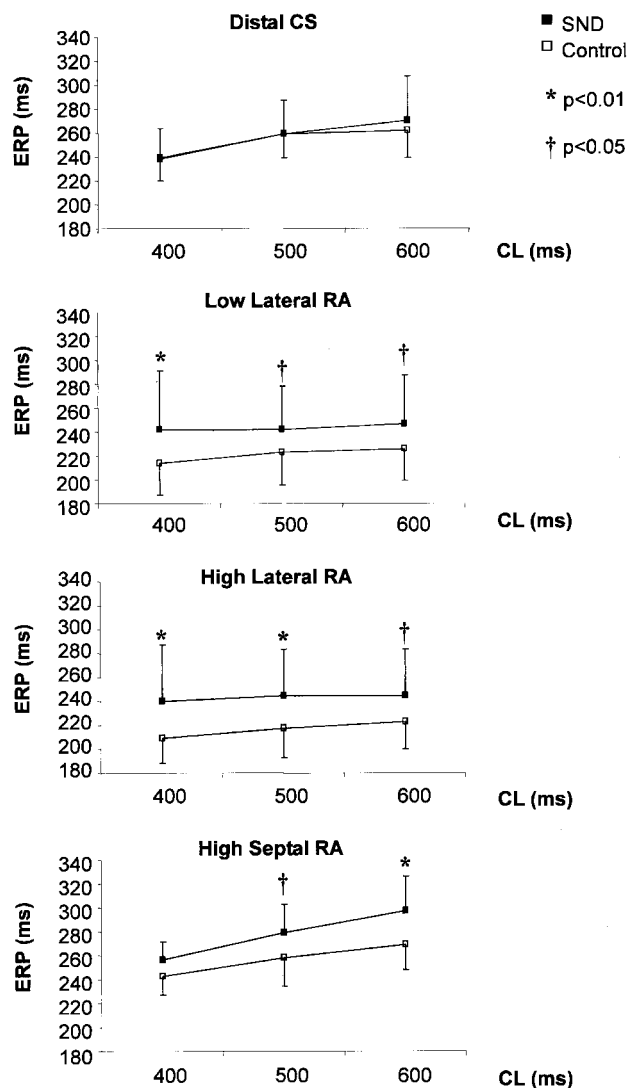

Figure 1. Atrial refractoriness.

400 ms at the high septal RA. In contrast, there was no significant change in ERPs at the distal CS at any of the CLs examined. The normal physiological rate adaptation of ERP was either reversed or attenuated at the high and low lateral RA while being maintained at the distal CS and high septal RA in patients with SND. There was no significant change in the heterogeneity of ERP at any of the CLs examined.

Atrial Conduction

There was significant prolongation in the atrial conduction time along the lateral RA catheter (bipole 1-2 to 9-10) in patients with SND compared with controls ($P < 0.0001$): at 600 ms, 48±5 versus 41±4 ms ($P < 0.01$); at 500 ms, 49±5 versus 39±5 ms ($P < 0.01$); and at 400 ms, 49±8 versus 41±6 ms ($P < 0.01$). Conduction time along the CS catheter (bipole 1-2 to 9-10) was also significantly prolonged in patients with SND compared with controls ($P < 0.0001$): at 600 ms, 39±5 versus 33±4 ms ($P < 0.01$); at 500 ms, 39±4 versus 32±4 ms ($P < 0.01$); and at 400 ms, 39±5 versus 33±5 ms ($P < 0.01$).
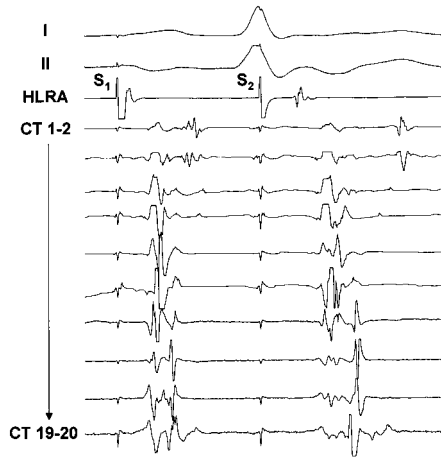
Figure 2. Electrograms along crista terminalis during last beat of drive train and extrastimulus from high lateral RA. Note DP, FS, and complex activation across this structure (all of which increase with extrastimulus).

## Anatomically Determined Conduction Delay

There was evidence of significant conduction delay along the crista terminalis in patients with SND, as evidenced by recordings on the crista terminalis catheter (Figure 2), with both a significantly greater number of DPs ($P<0.0001$) and a greater maximum interpotential distance ($P<0.0001$; Table 2). These changes were significantly greater during the drive and with the extrastimulus. With progressively earlier extrastimuli, there was an increase in the number and interpotential duration of DPs at the crista terminalis (Figure 3), supporting the notion that the delay at the crista terminalis was functional.

Electroanatomic Mapping

A mean of 267 ± 51 points per patient during pacing and 180 ± 51 points per patient during sinus rhythm were analyzed, with no significant difference in the number of points analyzed in each group.

Activation and Propagation Mapping in Sinus Rhythm

In 7 patients with SND who had stable rhythm with P-wave morphology consistent with a sinus node origin and 7
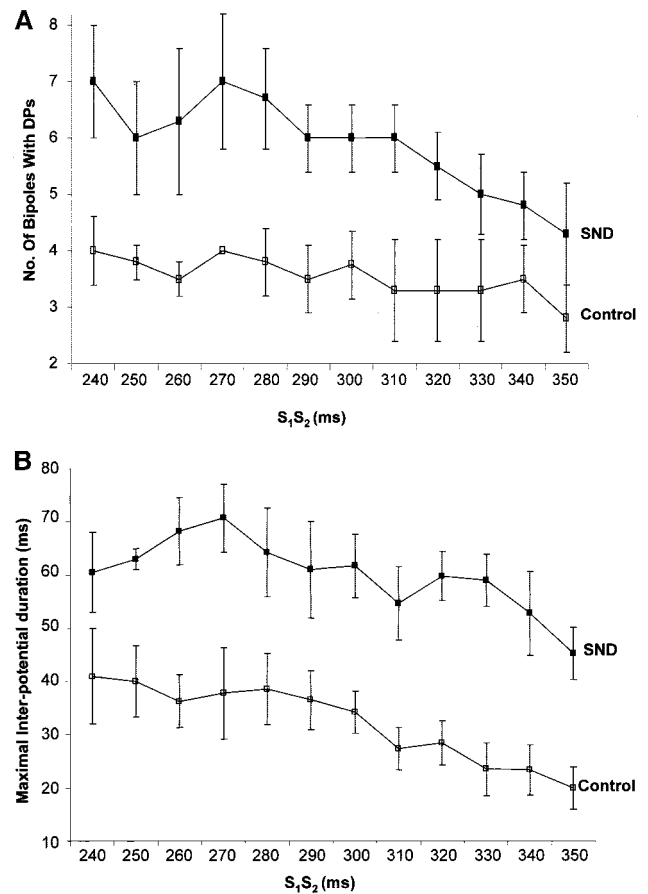
Figure 3. Crista terminalis conduction during decremented extrastimuli. A, Number of DPs. B, Maximum interpotential duration during decremented extrastimuli.

controls, activation mapping was performed in sinus rhythm at CLs of 1326 ± 664 and 733 ± 123 ms, respectively ($P=0.003$). Patients with SND demonstrated 1.6 ± 1.1 sinus activation sites, with unicentric activation in 5. These sites were separated by 4 ± 8 mm. In contrast, all 7 control patients demonstrated multicentric sinus node origin, with simultaneous activation of 3.6 ± 1.7 sites ($P=0.01$) separated by 27 ± 14 mm ($P=0.003$; Figure 4A).

TABLE 2.   Transverse Crista Terminalis Conduction

	S_1		S_2	
Site	Control	SND	Control	SND
No. of double potentials				
Low-lateral RA	1.4 ± 1.3	4.0 ± 2.7*	3.5 ± 1.8	8.0 ± 2.5*
High-lateral RA	2.3 ± 1.4	4.7 ± 2.7*	3.0 ± 1.7	7.5 ± 2.4*
High-septal RA	1.9 ± 2.3	4.0 ± 2.4*	3.3 ± 2.1	6.8 ± 2.0*
Maximum interpotential duration				
Low-lateral RA	20.4 ± 16.6	49.0 ± 12.5*	52.0 ± 25.5	76.3 ± 22.9*
High-lateral RA	28.3 ± 16.0	53.3 ± 15.5*	54.7 ± 21.9	88.2 ± 15.9*
High-septal RA	15.7 ± 21.0	45.8 ± 10.2*	39.1 ± 22.7	69.2 ± 25.0*

S_1 refers to the drive (600 ms) and S_2 refers to the first captured atrial extrastimulus using an incremental technique.

*$P<0.01$.
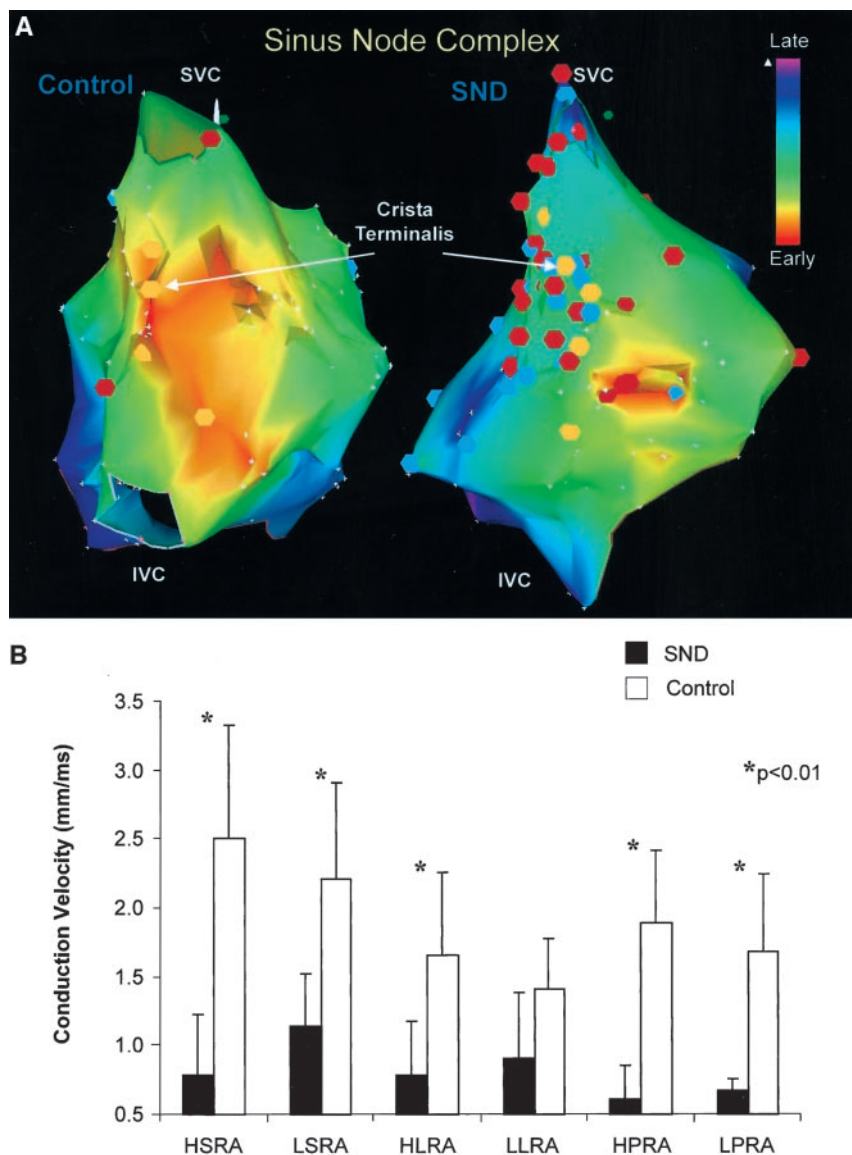
Figure 4. A, Activation mapping in sinus rhythm in a patient with SND (right) and an age-matched control (left). Both atria are oriented such that posterior RA (crista terminalis, shown in yellow dots) is en face to demonstrate sinus node complex. Patient with SND demonstrates significantly greater number of points with DP (blue dots) and FS (brown dots) and earliest activity (sinus node complex) over a greater extent of crista terminalis. B, Regional conduction velocity.

The sinus pacemaker complex was located significantly more caudally in patients with SND than in controls, the distance from the SVC to the most cranial pacemaker being 34 ± 16 and 9 ± 5 mm, respectively ($P=0.006$). In 5 of the 7 patients with SND, this focus of sinus node activity was located within the lower one third of the crista terminalis, whereas in all controls, sinus node activity was located in the superior two thirds or spanned most of the length of the crista terminalis (Figure 4A). In all patients with SND, the site of origin of the sinus impulse correlated with the region of largest residual voltage amplitude along the crista terminalis.

Propagation of the sinus impulse in patients with SND was observed to encounter areas of marked conduction delay and conduction block, particularly along the crista terminalis, resulting in circuitous depolarization wave fronts and regions of delayed atrial activation. In 5 of the 7 patients with SND, the sinus impulse was observed exiting to the atria at the anteroinferior margin of the crista terminalis (Figure 5A). Wave-front propagation was relatively rapid over the superoanterior wall. However, significantly delayed activation was observed over the crista terminalis in the septal direction, with the activation fronts breaking cranially, caudally, and through gaps along this anatomic structure (Figure 5A). The activation time from the earliest sinus impulse to the septal RA was significantly prolonged in patients with SND compared with controls (54 ± 15 versus 27 ± 11 ms, $P=0.008$). In addition, despite the significantly more caudal location of the sinus node complex in patients with SND, the activation time of the earliest sinus impulse to the inferior IVC-RA junction demonstrated a trend to be prolonged (56 ± 24 versus 34 ± 14 ms; $P=0.09$). In controls, the sinus node impulse exited simultaneously on either side of the crista terminalis, with rapid activation in both septal and anterior directions (Figure 5B).

Patients with SND demonstrated a significantly greater percentage of points with DPs ($29\pm10\%$ versus $2\pm2\%$, $P=0.002$) and FSs ($18\pm7\%$ versus $4\pm5\%$, $P=0.006$) compared with controls during sinus rhythm. These were widespread, with a concentration along the crista terminalis and the septal RA. In addition, there was significant prolongation
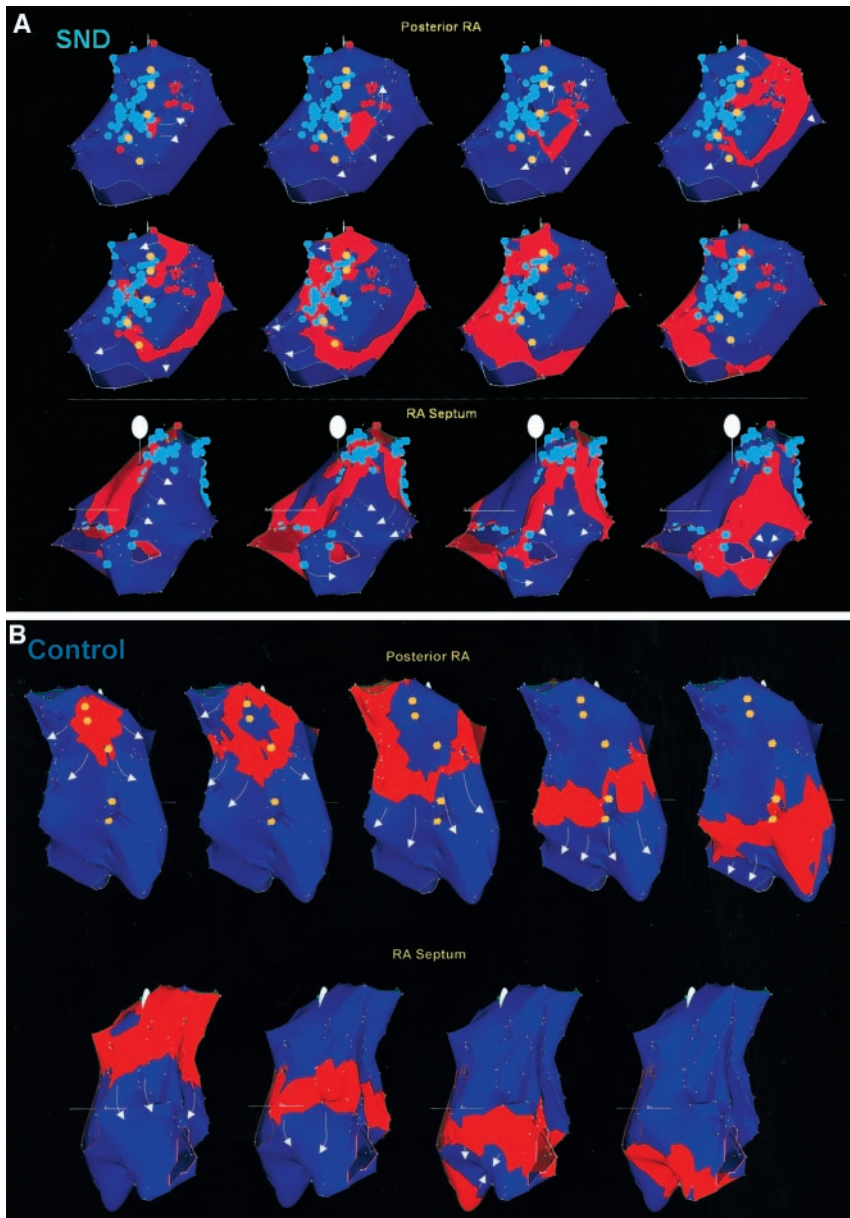
Figure 5. Propagation map during sinus rhythm in (A) SND and (B) control. There is simultaneous activation either side of crista terminalis (yellow dots). There are points demonstrating DP (blue dots) and FS (brown dots). See text for details.

of the RA activation time in patients with SND compared with controls in sinus rhythm (123±30 versus 98±9 ms; $P=0.02$).

### Activation Mapping During Atrial Pacing

In 9 patients with SND and 9 controls, activation mapping was performed during atrial pacing. During distal CS pacing, the earliest RA activity was at the CS ostium, with the RA being activated similarly in both groups. Regional atrial conduction velocity during atrial pacing was slower in all regions evaluated within the RA in patients with SND ($P<0.0001$; Figure 4B).

Patients with SND demonstrated significantly greater percentages of points with FS and DP compared with controls during atrial pacing (Figure 4A): 26±10% versus 10±2% ($P=0.0002$) and 14±7% versus 3±2% ($P=0.0007$), respectively.

Bipolar Voltage Mapping

Voltage mapping in patients with SND showed extensive regions of low voltage (≤0.5 mV) within the RA (Figure 6A). The mean RA bipolar voltage amplitude was significantly reduced in patients with SND both during sinus rhythm (1.3±0.5 versus 2.3±0.4 mV, $P=0.003$) and atrial pacing (1.1±0.2 versus 1.9±0.3 mV, $P<0.0001$) compared with controls.

At each RA region evaluated, there was a significantly reduced bipolar voltage in patients with SND compared with controls ($P<0.0001$; Figure 6B); this was most noticeable along the crista terminalis (posterior RA). There was also significantly greater heterogeneity of the voltage within the RA, as determined by the coefficient of variation in patients with SND compared with controls: 86±20% versus 64±10% ($P=0.03$) during sinus rhythm and 82±7% versus 60±6% ($P<0.0001$) during atrial pacing. In 7 of the 9 SND patients without stable underlying rhythm, there were areas of elec-
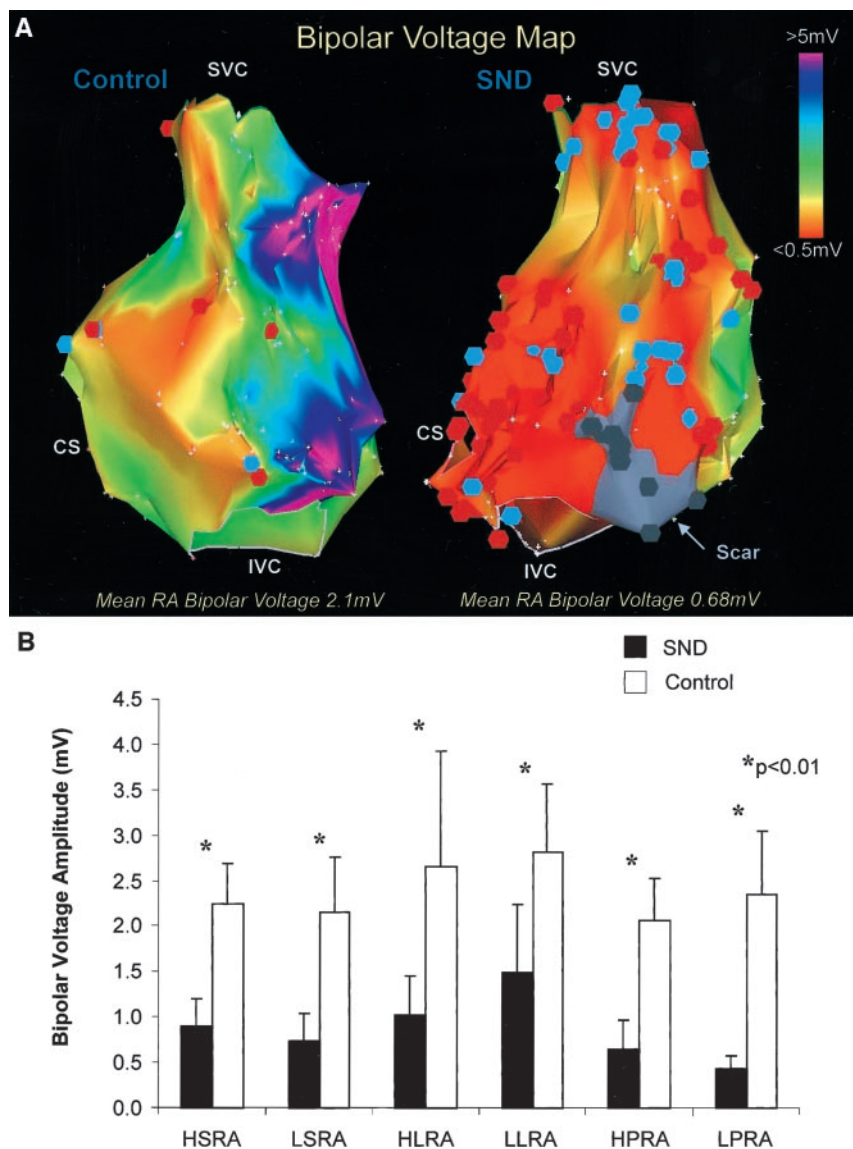
Figure 6. A, Bipolar voltage mapping in a patient with SND (right) and an age-matched control (left). Both atria are oriented such that posterior RA is en face. Areas of electrical silence (scar) are demonstrated in gray. Note, patient with SND demonstrates significantly greater number of points with DP (blue dots) and FS (brown dots). B, Regional bipolar voltage.

trical silence or scar at the low posteroseptal RA or low crista terminalis (Figure 6A), with 4 ± 1 points per patient representing regions of electrical silence. None of the control patients demonstrated any areas of electrical silence.

Discussion

This study presents new information regarding the electrophysiological and electroanatomic remodeling of the atria in patients with SND. Our findings demonstrate that SND is associated with widespread atrial abnormalities.

First, structural and anatomic abnormalities were observed. These patients demonstrated significant left atrial enlargement and evidence of loss of functioning atrial myocardium with regions of low voltage amplitude and spontaneous scarring. These regions of low voltage and scarring were particularly marked along the crista terminalis.

Second, patients with SND demonstrated widespread conduction abnormalities with both conventional and electroanatomic mapping. There was also anatomically determined functional conduction delay at the crista terminalis. These abnormalities resulted in propagation detours and colliding activation wave fronts of atrial activation.

Third, atrial ERP was increased at all RA sites, with loss of the normal physiological rate adaptation of ERP along the lateral RA but with no change in the heterogeneity of ERP.

Sinus Node Function

The work of Boineau and coworkers led to a paradigm shift in our understanding of the sinus node. Whereas histological studies had suggested a discrete and localized node in the epicardial region of the atrium at the SVC-RA junction, the elegant mapping studies of Boineau et al demonstrated that physiologically there was a diffuse and integrated pacemaker complex extending from the SVC-RA junction virtually to the IVC-RA junction and arranged along the long axis of the crista terminalis.[4,6] Although earliest activation in sinus rhythm may occur simultaneously from more than 1 site in this complex, sympathetic activation leads to dominance of faster cranial foci and vagal activation to slower more caudal foci.

We hypothesized that given the widely distributed nature of the pacemaker complex, significant derangements of sinus node function would require extensive loss of pacemaker automatic tissue and widespread impairment of sinoatrial conduction. Indeed, studies of sinus node modification and sinus node ablation have demonstrated that to modify or abolish sinus node function, an extensive region along the crista terminalis must be ablated.[11]

In the present study, patients with SND demonstrated evidence of extensive loss of normal tissue along the crista terminalis with low amplitude signals and regional scarring, suggesting loss of automatic pacemaker cells in this region. The normally multicentric sinus node complex was found to be unicentric, becoming localized to the region of largest residual voltage amplitude along the crista terminalis. In addition, the observed conduction abnormalities at the crista terminalis could potentially result in reentry and may be associated with impaired sinoatrial conduction.

Previous Studies of Atrial Abnormalities in SND

In contrast to the large number of studies using traditional indices of sinus node function in patients with SND, there is a relative paucity of information describing global RA electrophysiology in these patients. Several studies have indirectly suggested the presence of a widespread atrial process in SND. These have observed the occurrence of prolonged P-wave duration with prolonged and fractionated atrial electrograms.[12,13] These abnormalities have been observed during both sinus rhythm and atrial pacing, with a suggestion that patients who had associated AF had a wider distribution of abnormal atrial findings. De Sisti et al[14] retrospectively reviewed patients with SND who had electrophysiological assessment and found no change in ERP at the high RA at a CL of 600 ms but significant increase in electrogram duration both during the drive CL and extrastimulus compared with controls. However, the control group in that study was not age-matched and included patients with syncope or other conduction abnormalities.

Structural Abnormalities in the Atrium

The development of atrial structural abnormalities is now being increasingly recognized in a range of conditions affecting the atrium. There is evidence from both animal and human studies demonstrating that AF can lead to altered patterns of connexins, changes in myocyte cellular substructure, interstitial fibrosis, and apoptotic atrial myocyte death.[15] Similar observations of advanced structural abnormalities have also been observed in other conditions predisposing to sinus node dysfunction, such as congestive heart failure.[9,16]

In the present study, patients with SND and no previous arrhythmias demonstrated quite extensive structural abnormalities, as evidenced by low atrial voltage and areas of spontaneous scarring. Although these changes may be induced by factors such as chronic atrial stretch[17,18] and chronic atrial arrhythmias,[15] the mechanism of their occurrence in patients with SND is not known. Pathological studies of patients with SND have observed degeneration, fatty infiltration, and fibrosis of the sinus node region, but little is known of the remaining atria.[2] Similarly, a study of age-related changes in the region of the histological sinus node described an apparent loss of atrial muscle with an increase in connective tissue and fat in this region.[19] However, the marked contrast in findings between patients with SND and age-matched controls in the present study suggests that they cannot be attributed to the aging process alone.

Although these findings are similar to patients with congestive heart failure, whether similar consequences can be expected of all conditions predisposing to atrial arrhythmias is unknown.

SND and AF

The frequent association between SND and atrial arrhythmias has long been recognized and forms the basis of the tachycardia-bradycardia syndrome.[1] However, whether there is a primary causal relationship between these conditions is unclear. Evidence exists to support the argument that AF leads to sinus node dysfunction[20] via the phenomenon of sinus node remodeling and structural remodeling of the atrium, but others have suggested that the reverse occurs. Thus, the development of AF in SND has been attributed to bradycardia-related inhomogeneous refractoriness, which enhances the AF vulnerability of the atrium to atrial premature beats.[21]

The present study demonstrates that the primary underlying substrate for sinus node dysfunction includes abnormalities that might also predispose to AF. Thus, the development of slowed conduction, regional conduction block, and anatomic obstacles (electrical silence) with propagation detours in the context of atrial enlargement would be expected to predispose to maintenance of multiple wavelet reentry.

Study Limitations

Whether the abnormalities observed in the RA of patients with SND are responsible for the increased incidence of clinical AF in these patients remains speculative, because patients with previous AF were necessarily excluded from the study. Importantly, the development of clinical AF is complex and depends not only on the substrate but also on other factors, such as triggers and initiators that were not addressed by this study.

Conclusions

This study demonstrates that patients with SND have evidence of diffuse atrial abnormalities characterized by (1) anatomic and structural abnormalities, including atrial enlargement, regions of low voltage, and scarring; (2) widespread conduction slowing and anatomically determined conduction delay; and (3) increased right atrial refractoriness.

These abnormalities were associated with a change in the nature of sinus pacemaker activity with loss of the normal multicentric pattern of onset, shift of the pacemaker complex to low crista terminalis sites, and the presence of abnormal and circuitous conduction around lines of conduction block.

References

1. Ferrer MI. The sick sinus syndrome in atrial disease. *JAMA*. 1968;206: 645–646.
2. James TN. The sinus node. *Am J Cardiol*. 1977;40:965–986.
3. Boineau JP, Schuessler RB, Hackel DB, et al. Widespread distribution and rate differentiation of the atrial pacemaker complex. *Am J Physiol*. 1980;239:H406–H415.
4. Boineau JP, Schuessler RB, Roeske WR, et al. Quantitative relation between sites of atrial impulse origin and cycle length. *Am J Physiol*. 1983;245:H781–H789.
5. Boineau JP, Miller CB, Schuessler RB, et al. Activation sequence and potential distribution maps demonstrating multicentric atrial impulse origin in dogs. *Circ Res*. 1984;54:332–347.
6. Boineau JP, Canavan TE, Schuessler RB, et al. Demonstration of a widely distributed atrial pacemaker complex in the human heart. *Circulation*. 1988;77:1221–1237.
7. Kall JG, Rubenstein DS, Kopp DE, et al. Atypical atrial flutter originating in the right atrial free wall. *Circulation*. 2000;101:270–279.
8. Jais P, Shah DC, Haissaguerre M, et al. Mapping and ablation of left atrial flutters. *Circulation*. 2000;101:2928–2934.
9. Sanders P, Morton JB, Davidson NC, et al. Electrical remodeling of the atria in congestive heart failure: electrophysiological and electroanatomic mapping in humans. *Circulation*. 2003;108:1461–1469.
10. Prystowsky EN, Jackman WM, Rinkenberger RL, et al. Effect of autonomic blockade on ventricular refractoriness and atrioventricular nodal conduction in humans: evidence supporting a direct cholinergic action on ventricular muscle refractoriness. *Circ Res*. 1981;49:511–518.
11. Kalman JM, Lee RJ, Fisher WG, et al. Radiofrequency catheter modification of sinus pacemaker function guided by intracardiac echocardiography. *Circulation*. 1995;92:3070–3081.
12. Liu Z, Hayano M, Hirata T, et al. Abnormalities of electrocardiographic P wave morphology and their relation to electrophysiological parameters of the atrium in patients with sick sinus syndrome. *Pacing Clin Electrophysiol*. 1998;21:79–86.
13. Centurion OA, Isomoto S, Fukatani M, et al. Relationship between atrial conduction defects and fractionated atrial endocardial electrograms in patients with sick sinus syndrome. *Pacing Clin Electrophysiol*. 1993;16: 2022–2033.
14. De Sisti A, Leclercq JF, Fiorello P, et al. Electrophysiologic characteristics of the atrium in sinus node dysfunction: atrial refractoriness and conduction. *J Cardiovasc Electrophysiol*. 2000;11:30–33.
15. Ausma J, Wijffels M, Thone F, et al. Structural changes of atrial myocardium due to sustained atrial fibrillation in the goat. *Circulation*. 1997; 96:3157–3163.
16. Li D, Fareh S, Leung TK, et al. Promotion of atrial fibrillation by heart failure in dogs: atrial remodeling of a different sort. *Circulation*. 1999; 100:87–95.
17. Sparks PB, Mond HG, Vohra JK, et al. Electrical remodeling of the atria following loss of atrioventricular synchrony: a long-term study in humans. *Circulation*. 1999;100:1894–1900.
18. Morton JB, Sanders P, Vohra JK, et al. The effect of chronic atrial stretch on atrial electrical remodeling in patients with an atrial septal defect. *Circulation*. 2003;107:1775–1782.
19. Lev M. Aging changes in the human sinoatrial node. *J Gerontol*. 1954; 9:1–9.
20. Elvan A, Wylie K, Zipes DP. Pacing-induced chronic atrial fibrillation impairs sinus node function in dogs: electrophysiological remodeling. *Circulation*. 1996;94:2953–2960.
21. Luck JC, Engel TR. Dispersion of atrial refractoriness in patients with sinus node dysfunction. *Circulation*. 1979;60:404–412.

Electrophysiological and Electroanatomic Characterization of the Atria in Sinus Node Disease: Evidence of Diffuse Atrial Remodeling

Prashanthan Sanders, Joseph B. Morton, Peter M. Kistler, Steven J. Spence, Neil C. Davidson, Azlan Hussin, Jitendra K. Vohra, Paul B. Sparks and Jonathan M. Kalman

The online version of this article, along with updated information and services, is located on the
World Wide Web at:
http://circ.ahajournals.org/content/109/12/1514